molecular oral microbiology

molecular oral microbiology

Identification of a functional capsule locus in *Streptococcus mitis*

H.V. Rukke[1], I.K. Hegna[2] and F.C. Petersen[1]

1 Department of Oral Biology, Faculty of Dentistry, University of Oslo, Oslo, Norway
2 Department of Pharmaceutical Biosciences, School of Pharmacy, University of Oslo, Oslo, Norway

Correspondence: Håkon Valen Rukke, Department of Oral Biology, Faculty of Dentistry, University of Oslo, PO Box 1052, Blindern, N0316 Oslo, Norway Tel.: +47 2284 0366; fax: +47 2284 0302; E-mail: h.v.rukke@odont.uio.no

Keywords: biofilm; capsule; mitis group; *Streptococcus*
Accepted 10 November 2011
DOI: 10.1111/j.2041-1014.2011.00635.x

SUMMARY

The polysaccharide capsule of *Streptococcus pneumoniae* is a hallmark for virulence in humans. In its close relative *Streptococcus mitis*, a common human commensal, analysis of the sequenced genomes of six strains revealed the presence of a putative capsule locus in four of them. We constructed an isogenic *S. mitis* mutant from the type strain that lacked the 19 open reading frames in the capsule locus (Δ*cps* mutant), using a deletion strategy similar to previous capsule functional studies in *S. pneumoniae*. Transmission electron microscopy and atomic force microscopy revealed a capsule-like structure in the *S. mitis* type strain that was absent or reduced in the Δ*cps* mutant. Since *S. mitis* are predominant oral colonizers of tooth surfaces, we addressed the relevance of the capsule locus for the *S. mitis* overall surface properties, autoaggregation and biofilm formation. The capsule deletion resulted in a mutant with approximately two-fold increase in hydrophobicity. Binding to the Stains-all cationic dye was reduced by 40%, suggesting a reduction in the overall negative surface charge of the mutant. The mutant exhibited also increased autoaggregation in coaggregation buffer, and up to six-fold increase in biofilm levels. The results suggested that the capsule locus is associated with production of a capsule-like structure in *S. mitis* and indicated that the *S. mitis* capsule-like structure may confer surface attributes similar to those associated with the capsule in *S. pneumoniae*.

INTRODUCTION

Streptococcus mitis, a member of the mitis group of streptococci, colonizes virtually all surfaces of the oral cavity, including teeth, tongue, and mucosal surfaces, as well as the tonsils and nasopharynx (Pearce *et al.*, 1995; Aas *et al.*, 2005). It is also one of the first bacteria to colonize the oral cavity of newborns (Pearce *et al.*, 1995), and one of the few in the oral cavity of adults with the ability to colonize the teeth at early stages of dental plaque formation (Pearce *et al.*, 1995; Li *et al.*, 2004). Early colonizers such as *S. mitis* are thought to form the basis to which secondary colonizers may adhere in the developing oral biofilms (Kolenbrander & London, 1993). Although most often found as commensals in the human host, alarming cases of septicaemia in neutropenic cancer patients following chemotherapy have been reported (Beighton *et al.*, 1994; Marron *et al.*, 2000; Tunkel & Sepkowitz, 2002). *Streptococcus mitis* is also one of the most common oral streptococci associated with endocarditis (Levitz, 1999; Sabella *et al.*, 2001).

A close relative of *S. mitis* is *Streptococcus pneumoniae*, also a member of the mitis group of streptococci (Kilian *et al.*, 2008). The pathogenic potential of *S. pneumoniae* is, however, by far more significant, killing approximately one and a half million people every year worldwide (Kadioglu *et al.*, 2008). Both *S. mitis* and *S. pneumoniae* are thought to have evolved from a common ancestor that closely resembled the present *S. pneumoniae*. It is purported, further, that in *S. mitis* loss of virulence determinants may have led to a reduction in pathogenic potential, compared with *S. pneumoniae* and their common ancestor (Kilian *et al.*, 2008). The differences in pathogenicity between *S. mitis* and *S. pneumoniae* are, however, striking considering that the genomes of *S. mitis* strains reveal the presence of up to 83% of *S. pneumoniae* virulence genes (Johnston *et al.*, 2010). Among the homologous genes associated with virulence are those found in the capsule loci (Kilian *et al.*, 2008; Johnston *et al.*, 2010).

Capsule production is a hallmark of virulence in *S. pneumoniae* and the loss of capsule makes *S. pneumoniae* virtually avirulent (MacLeod & Krauss, 1950; Kim & Weiser, 1998). In *S. pneumoniae* more than 90 different serotypes have been identified, that differ in their abilities to colonize and cause disease (Bogaert *et al.*, 2004; Weinberger *et al.*, 2009). The *S. pneumoniae* capsule serves important functions such as protecting *S. pneumoniae* from complement-mediated opsonophagocytosis (Kim *et al.*, 1999), and hindering *S. pneumoniae* from being trapped in the respiratory tract mucus (Nelson *et al.*, 2007). In epithelial adhesion and transmigration models, acapsular variants of *S. pneumoniae* adhere and internalize at higher numbers to epithelial cells (Hammerschmidt *et al.*, 2005, 2007), and exhibit an increased migration rate across epithelium (Beisswenger *et al.*, 2007). Regulation of capsule production is thought to play an important role in colonization, with increased production favouring protection against host defences, whereas reduced production may favour adherence (Hammerschmidt *et al.*, 2005). In addition, capsule expression influences the overall surface properties (Granlund-Edstedt *et al.*, 1993; Swiatlo *et al.*, 2002), as well as the growth rate (Pearce *et al.*, 2002) and biofilm formation of *S. pneumoniae* (Munoz-Elias *et al.*, 2008).

Polymerase chain reaction (PCR) amplification of possible capsule-encoding regions indicates that the capsule locus may be widely present in *S. mitis* (Kilian *et al.*, 2008), but it is not known whether different capsule types are likely to be found in *S. mitis*, or whether the locus is functional in *S. mitis*. The possibility that a functional capsule locus may also be present in *S. mitis* is likely to have important implications for our understanding of the molecular strategies used by *S. mitis* to successfully colonize the host.

The aim of this study was to investigate whether the capsule biosynthetic locus was associated with the production of a capsule-like structure on the surface of *S. mitis*, and whether deletion of the locus may affect *S. mitis* overall surface characteristics, autoaggregation and biofilm formation.

METHODS

Bacteria and culture

The *S. mitis* CCUG 31611 type strain (NCTC 12261) and the isogenic mutants used in this study are shown in Table 1. The bacteria were stored at −80°C in Todd–Hewitt broth (THB, Becton Dickinson and Company, Le Pont de Claix, France) supplemented with 15% glycerol. For functional and transformation assays, as well as for transmission electron microscopy (TEM) the bacteria were grown in tryptic soy

Table 1 Primers, strains and competence stimulating peptides used in this study

Primers[1]	
FP369	GCCGTTCGTGGTATGAGTCG
FP370	GGTCGCAACTGTGCGCTTAC
FP475	TTTTTAGCGCCAACACCAG
FP476	AGGCGCGCCTTGTGAGATAAATCCGCTTAGG
FP477	AGGCCGGCCTGACAACAGCTTTGCAGTGT
FP47S	ATAAGCATCCAGCCCCTTG
FP635	GACCAAGAATACCGC GAAAA
FP636	TTGGTCATCCCAATCTCCTC
FP637	GAAGAGTACGCCCCAGTCAA
FP638	TCAAGCCCTTGATCGAGTTT
FP639	GTCTTAGCG6CTTGTTCTGG
FP640	GAAGTAGCTGCCTTGCTGGT
Strains	
MIWT WT *Streptococcus mitis* CCUG 31611	
MI015 MIWT, but Δcps::PcEm, Em^R	
MI016 MIWT, but Δcps::PcKan, Kan^R	
Copetence stimulating peptide	
GEIRQTHNIFFNFFKRR	

[1]Restriction sites are underlined: *Asc*I GG/CGCGCC, *Fse*I GGCCGG/CC.

broth (TSB, Oxoid, Hampshire, UK). For atomic force microscopy (AFM) the strains were grown on blood agar base No. 2 (Oxoid) supplemented with 5% defibrinated sheep blood (TCS Biosciences Ltd., Buckingham, UK). Incubation was conducted at 37°C in normal or 5% CO_2-supplemented atmosphere. To prepare the pre-cultures used in the transformation experiments (see below) *S. mitis* was incubated at 37°C in THB for 16 h overnight in 5% CO_2-supplemented atmosphere, followed by a 1 : 25 dilution in THB. The diluted cultures were then grown until they reached an absorbance of 0.3 at 600 nm (OD_{600}, Biophotometer; Eppendorf, Hamburg, Germany), at which point the cells were stored at −80°C in 15% glycerol. For the selection of mutants, kanamycin was used at a final concentration of 500 μg ml^{-1}, and erythromycin at a final concentration of 10 μg ml^{-1}.

Construction of mutants

We used genomic tools at CMR (http://www.cmr.jcvi.org) to identify the capsule locus in the *S. mitis* type strain CCUG 31611, and the flanking genes *aliB* and *aliA*. The capsule locus was deleted using the PCR ligation mutagenesis strategy (Lau *et al.*, 2002; Pearce *et al.*, 2002). Briefly, we amplified flanking regions of the capsule locus using primer pairs FP475–FP476 and FP477–FP478 (Table 1). The *S. mitis* PCR products were ligated with T4 DNA ligase (Fermentas, St Leon, Germany) to a kanamycin cassette without terminal (Petersen *et al.*, 2005) or an erythromycin cassette with terminal (Lee & Morrison, 1999), and PCR amplified with the use of primer pairs FP475–FP478 (Table 1). The PCR products were purified using a PCR purification kit (Qiagen, Hilden, Germany) and used to transform the *S. mitis* wild-type.

Transformation

Transformation was carried out as described by Petersen & Scheie (2010) with slight modifications. Briefly, pre-cultures of *S. mitis* were diluted 1 : 10 in TSB. Competence stimulating peptide (Genescript inc, NJ; Table 1) was added at a final concentration of 125 nM. For the transformation and the construction of the Δ*cps* mutants 15 μl of the PCR ligation products was used. The cultures were incubated at 37°C in normal atmosphere for 4 h. Mutants were selected on blood agar plates supplemented with the appropriate antibiotics. Three colonies were selected for further studies, and deletion was verified with PCR and gel electrophoresis.

Real time reverse transcription-PCR

Total RNA from *S. mitis* wild-type and the Δ*cps* mutant grown in TSB was extracted at late-exponential phase with the High pure RNA isolation kit (Roche, Manheim, Germany) according to the manufacturer's recommendation, except that the cells were incubated at 37°C for 20 min in 200 μl lysis buffer containing 20 mg lysozyme ml^{-1} and 100 U mutanolysin ml^{-1}. DNaseI was used during the RNA extraction to remove remaining DNA. Complementary DNA templates were prepared from RNA using the Transcriptor First Strand cDNA Synthesis Kit (Roche Diagnostics GmbH, Mannheim, Germany) following the manufacturer's protocol. Controls without reverse transcriptase were included. Expression of the flanking genes *dexB*, *aliB* and *aliA* were examined by real-time PCR using the primer pairs FP635–FP636, FP637–FP638, and FP639–FP640, respectively. To normalize the data, the primer pair FP369–FP370 was used to amplify a sequence in *gyrA*. Assays were carried out using the Stratagene MX 3005 PCR system (Stratagene, La Jolla, CA, USA) using qPCR Mastermix for SYBR Green I (Eurogentec, Liège, Belgium). The gradient thermocycling programme was set for 40 cycles of 95°C for 15 s, 58°C for 30 s and 72°C for 30 s, with an initial cycle at 95°C for 10 min. During each cycle, the accumulation of PCR products was detected by monitoring the increase in fluorescence of the reporter dye from double-stranded-DNA-binding SYBR green. Dissociation curves were run immediately after the last PCR cycle by plotting the fluorescence intensities against temperatures as the set-point temperatures (55°C) were increased by 1°C for 30 s (41 cycles). Data were collected and compared using the software and graphics program MXPRO (Stratagene). Primer pair efficiencies were calculated using MXPRO software (Stratagene) (Table 1), and relative expression data was analysed using REST 2005 software (Pfaffel et al., 2002).

Transmission electron microscopy

The procedure followed the lysine-acetate-based formaldehyde–glutaraldehyde ruthenium red–osmium fixa-

tion method, as described by Hammerschmidt *et al.* (2005). Briefly, *S. mitis* wild-type and Δ*cps* were grown in TSB overnight at 37°C in a 5% CO_2-supplemented atmosphere. The bacteria were centrifuged (5000 ***g***, 4°C, 10 min) and washed twice with phosphate-buffered saline (PBS), and then fixed with 2% formaldehyde and 2.5% gluteraldehyde in cacodylate buffer with 0.075% ruthenium red and 0.075 M lysine acetate for 20 min. The initially fixed samples were washed with cacodylate buffer with 0.075% ruthenium red, before a second fixation with 2% formaldehyde and 2.5% gluteraldehyde in cacodylate buffer with 0.075% ruthenium red for 3 h. The samples were then washed once again with cacodylate buffer containing 0.075% ruthenium red, followed by a third fixation step with 1% osmium in cacodylate buffer containing 0.075% ruthenium red for 1 h. The samples were finally embedded in Epon 100 (Agar Scientific, Stansted, UK) according to standard procedures, before ultrathin sections were cut and counterstained with 4% aqueous uranyl acetate for 5 min. The samples were examined with the CM 120 transmission electron microscope (Philips, Eindhoven, the Netherlands), and images were taken with a Morada camera on the iTEM platform (Soft Imaging System, Münster, Germany).

Atomic force microscopy

Streptococcus mitis wild-type and Δ*cps* were grown overnight on blood agar in a 5% CO_2-supplemented atmosphere. The samples for AFM imaging were prepared by transferring colonies to 500 μl sterile filtered 2 mM HEPES (Gibco, CA) to make a homogeneous suspension of bacteria in HEPES. An optical microscope was used to establish an acceptable concentration of cells, before a 10-μl aliquot was transferred to a freshly cleaved mica. The samples were incubated at room temperature for 15 min, followed by a wash with 10 × 200 μl 2 mM HEPES. The samples were then dried by applying a soft jet stream of nitrogen. AFM imaging was performed in intermittent contact mode in air using the NanoWizard instrument from JPK (Berlin, Germany). The scanning probes used were NSC35/AlBS purchased from MicroMash (Estonia).

Stains-all assay

The assay was performed according to Hammerschmidt *et al.* (2005). The bacteria were grown under the same conditions as the microbial adhesion to hydrocarbons assay described below. At stationary phase 5 ml of the cultures was transferred to 14 ml Falcon tubes and centrifuged (5000 ***g***, 4°C, 10 min). The supernatants were then transferred to new tubes, and the pellets were washed twice with PBS, before diluting in 500 μl distilled water. A volume of 250 μl of supernatants of resuspended bacteria was then transferred to Eppendorf tubes, before adding 1 ml Stains-all solution [(20 mg Stains-all; Sigma, St Louis, MO), 60 μl glacial acetic acid (Merck, Darmstadt, Germany), and 100 ml 50% formamide (Sigma)]. The absorbance of the samples at 640 nm was then measured (GENESYS 10vis; Thermo, WI) and subtracted from the values of a negative control (distilled water or TSB with Stains-all).

Microbial adhesion to hydrocarbons

The microbial adhesion to hydrocarbons (MATH) assay was performed according to Rosenberg *et al.* (1980) with slight modification. Briefly, *S. mitis* wild-type and Δ*cps* were grown in THB at 37°C overnight in normal atmosphere or in 5% CO_2-supplemented atmosphere. They were then diluted 1 : 80 and grown until stationary phase under their respective atmospheric conditions. The bacteria were then centrifuged (5000 ***g***, 4°C, 10 min) and washed twice with PBS. The cell pellets were resuspended in PBS to OD_{600} 1.0 (A_0) (Biophotometer; Eppendorf, Hamburg, Germany), and 1.2 ml were transferred to Eppendorf tubes. A volume of 150 μl hexadecane (Sigma) was then added and the samples were incubated at 30°C for 10 min. After incubation the samples were vortexed vigorously, and left at room temperature for 15 min. Aliquots of 900 μl from the aqueous phase were then transferred to 1-ml cuvettes and the absorbance at OD_{600} was measured (A_1). The values were subtracted from measurements of a negative control with only PBS. The percentage of adhered bacteria to hexadecane was calculated by the equation: % adhesion to hexadecane = $[1-(A_0/A_1) \times 100]$.

Growth curve

Streptococcus mitis wild-type and the Δ*cps* mutant were grown overnight in a 5% CO_2-supplemented atmosphere. The overnight cultures were then

diluted 1 : 80, and 500 μl were distributed into wells of a 48-well plate (Nunclone, Roskilde, Denmark) before being incubated at 37°C in normal atmosphere or 5% CO_2-supplemented atmosphere. Absorbance at OD_{600} was measured at various time points using a Synergy HT Multi-Detection Microplate Reader (Biotek, Winooski, VT), until reaching the stationary growth phase. Values obtained with TSB alone were subtracted from the sample values.

Biofilm assay

Streptococcus mitis wild-type and the Δ*cps* mutant were grown to stationary phase as described above for the MATH and the Stains-all assays. The cultures were then diluted 1 : 75 in TSB (Oxoid) and 3 ml was transferred to each well of a 12-well mutidish polystyrene plate (Nunclone). To investigate biofilm formation under different atmospheric conditions, the plates were incubated at 37°C overnight either in normal atmosphere or 5% CO_2-supplemented atmosphere. Biofilm quantity was assessed after removing non-adherent cells by washing the wells twice with PBS. One millilitre of 0.1% safranin (BDH Chemicals, Poole Dorset, UK) was then added to each well and the plates were incubated at room temperature for 5 min. The stained biofilms were washed twice with PBS and left to dry at room temperature. The bound safranin was then released from the biofilms using 1 ml 30% glacial acetic acid (Merck) in each well. A volume of 200 μl was transferred to the wells of a 96-well microtiter plate, and optical density was measured at 530 nm in a Synergy HT Multi-Detection Microplate Reader.

Scanning electron microscopy of biofilms

The biofilms were visualized using scanning electron microscopy (SEM). Biofilms were grown in 12-well microtiter plates as described above, except that polystyrene discs (Nunclone) were immersed in the wells before inoculation. After rinsing, the biofilms were fixed with 2.5% glutaraldehyde in 0.1 M Sørensen buffer. Samples were dehydrated by rinsing the disks in ethanol, followed by critical point drying with liquid CO_2 and sputter coating with palladium/gold. Images were acquired using an XL30 Electron SEM model (Model XL 30 ESEM; Philips).

Autoaggregation

The autoaggregation assay was performed according to Cisar *et al.* (1979), except that the measured outcome was autoaggregation, instead of coaggregation. In brief, the coaggregation buffer (CAB) was made of 1 mM Tris–HCl pH 8.0, 0.1 mM $CaCl_2$, 0.1 mM $MgCl_2$, 0.15 M NaCl and sterile water. Overnight cultures of *S. mitis* wild-type and Δ*cps* were centrifuged (5000 ***g***, 4°C, 10 min) and washed twice with PBS, and resuspended in CAB to OD_{600} 0.650 (Biophotometer; Eppendorf). A volume of 2 ml bacterial suspension was then transferred to glass tubes and left at room temperature for approximately 10 min. Aliquots of 5 μl were placed on glass microscope slides and observed under phase contrast with a Nikon eclipse 600 microscope (Nikon Instruments Inc., Melville, NY). Images were taken with an Olympus UC30 (Olympus, Melville, NY) camera. Autoaggregation was also assessed by optical density measurements (Macfarlane *et al.*, 2008) taken immediately after resuspension in CAB and after 20 min.

Statistical analysis

One-way analysis of variance followed by the Holm–Sidak test was used for multiple comparisons, with a significance level set $P < 0.001$.

RESULTS

Analysis of the *S. mitis* capsule locus

Genomic sequences for six *S. mitis* strains are now available. Analysis of these reveals a putative capsule locus in four of the strains, including ATCC 6249 (GI306830256), SK 564 (GI307710678), SK 597 (GI307705952) and the type strain CCUG 31611 (NCTC12261; GI307708845) used in this study for further characterization (Fig. 1). Syntenic region analysis was performed with GEVO http://synteny.cnr.berkeley.edu/CoGe/GEvo.pl (Lyons & Freeling, 2008). The results revealed that *cpsA*, *cpsB*, *cpsC*, *cpsD* and *cpsE*, which are the first five genes in the *S. mitis* capsule locus, are arranged in the same order as in most *S. pneumoniae* and *Streptococcus oralis* (Mavroidi *et al.*, 2007; Kilian *et al.*, 2008). In the four *S. mitis* strains with a putative capsule locus, the locus is flanked upstream by *aliB* and down-

Figure 1 Gene organization of the capsule locus in *Streptococcus mitis* NCTC 12261^T (corresponds to CCUG 31611^T; GI307708845) compared with the three other sequenced *S. mitis* strains that also have capsule locus, SK 597 (GI307705952), ATCC 6249 (GI306830256) and SK 564 (GI307710678). Analysis was performed using GeVo at http://synteny.cnr.berkeley.edu/CoGe/GEvo.pl. The horizontal bars above the illustrated genes correspond to conserved gene sets between the *S. mitis* type strain and the other strains examined (light brown: homology with SK597; medium brown: homology with ATCC 6249; dark brown: homology with SK564). The vertical lines correspond to syntenic gene sets within the strain-specific region of the capsule locus. The open reading frames in the *S. mitis* type strain capsule locus encode genes with putative functions involved in regulation (*cps*A, *cps*B, *cps*C, *cps*D), transferase activity (SMT0219–SMT0225, SMT0228, and SMT0229), flippase (SMT0226), a UDP-galactofuranose mutase (SMT0227), and those participating in rhamnose synthesis (SMT0230–SMT0233).

stream by *aliA*. A homologue to the *dexB* encoding a glucan 1,6-α-glucosidase is found directly upstream of the *aliB* gene in all four *S. mitis* strains with a capsule locus. This organization is found in the unencapsulated *S. pneumoniae* BS 293, BS 455 and BS 457. In *S. oralis* ATCC 35037 the *dexB* gene is located in a different region of the genome then the capsule locus, whereas *aliB* is found directly upstream of *cpsA*. Similar to *S. pneumoniae* and *S. oralis*, the genes downstream of the *S. mitis cpsE* gene encode putative strain-specific enzymes (Mavroidi *et al.*, 2007; Kilian *et al.*, 2008). In this region homologues to the flipase Wzx and the polymerase Wzy, also found in all *S. pneumoniae* serotypes except serotype 3 and 37, are reported (Bentley *et al.*, 2006). The *S. mitis* B6 (Denapaite *et al.*, 2010) and SK 321 (GI 307711418) have homologues to *dexB* and *aliB*, but have no identifiable capsule locus between these genes.

Capsule locus deletion in *S. mitis* type strain

The *S. mitis* Δ*cps* mutant was constructed by allelic replacement of the capsule locus with a kanamycin or an erythromycin cassette. The deletion was verified by PCR, using primers complementary to the capsule locus flanking sequences *aliB* and *aliA* in *S. mitis* (FP475–FP478). The expected sizes of the amplified products, 2229 bp for the erythromycin construct and 2237 bp for the kanamycin construct were

confirmed by gel electrophoresis. Real-time reverse transcription-PCR was used to investigate the possibility of polar effects resulting in inactivation of the flanking genes *dexB*, *aliB* and *aliA*. The primer pairs used are shown in Table 1. The results indicated that the expression of the flanking genes *dexB*, *aliB* and *aliA* in the mutants was not significantly different from the wild-type constructed with either the kanamycin or the erythromycin cassettes. The confidence intervals for *dexB*, *aliB* and *aliA* were (0.55–1.6), (1.2–1.5) and (2.2–5.2) in the kanamycin construct, and (0.2–1.2), (0.6–2.4) and (0.7–2) in the erythromycin construct, respectively. The primer pair efficiencies were 95.5, 94.5 and 89.9%, respectively.

Visualization of *S. mitis* capsule-like structure by TEM and AFM

Transmission electron microscopy of *S. mitis* wild-type showed a capsule-like structure that was not found in the Δ*cps* mutant (Fig. 2). This structure resembled those illustrated for some *S. pneumoniae* (Hammerschmidt *et al.*, 2005). By using AFM with intermittent contact mode in air, more complex structures were revealed. Capsule-like structure was observed in the wild-type and to a lesser extent in the Δ*cps* mutant (Fig. 3). In certain regions, long fibril-like structures were found associated with the bacterial surfaces, which were apparently embedded in the capsule material (Fig. 3) Using HEPES in the sample preparation and washing of mica was crucial for AFM capsule visualization. The capsule-like material was absent or partially removed when 10 mM Tris–Mg^{2+} was used in the sample preparation and mica was washed with sterile filtered milliQ water.

Capsule-like production under growth in normal atmosphere supplemented or not with 5% CO_2

To start addressing the significance of the capsule-like structure to the *S. mitis* net-surface charge, and the possible role of environmental factors in *S. mitis* capsule-like production, we measured the ability of *S. mitis* to bind Stains-all during growth in normal or 5% CO_2-supplemented atmosphere. The two different conditions were chosen because atmospheric variations are likely to be found in oral biofilms *in vivo*. Stains-all is a cationic dye that binds to negatively charged molecules, such as those commonly found in capsule polysaccharides. The Δ*cps* mutant bound approximately 40% less of the dye than the wild-type, an effect that was not dependent on the CO_2 concentration (Fig. 4A). In the supernatants the values were below background levels, with similar values between the Δ*cps* mutant and the wild-type (data not shown). The results indicate, therefore, that the polysaccharides were mostly associated with the bacterial surface.

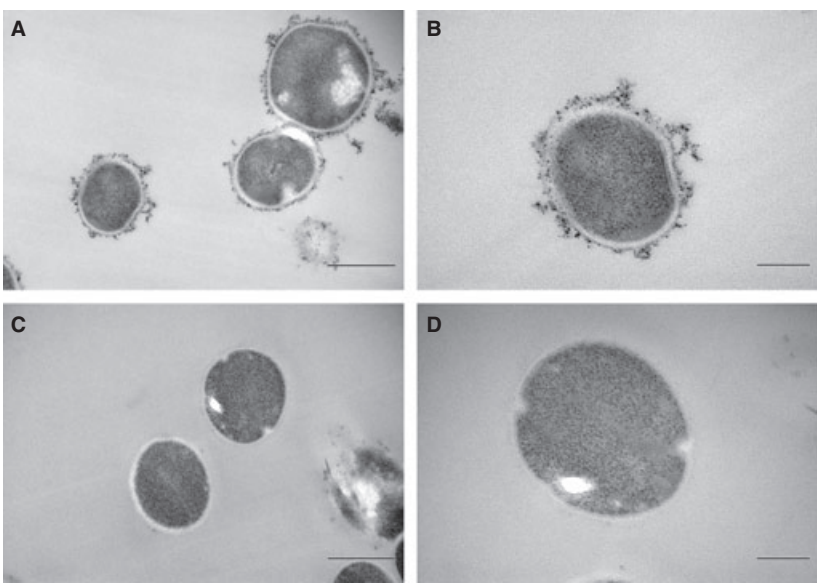

Figure 2 Capsule visualization using transmission electron microscopy. (A, B) The wild-type with the presence of capsule and (C, D) the MI016 Δ*cps* mutant is shown at two magnifications. Bars correspond to 0.5 μm (A, C), or to 0.2 μm (B, D).

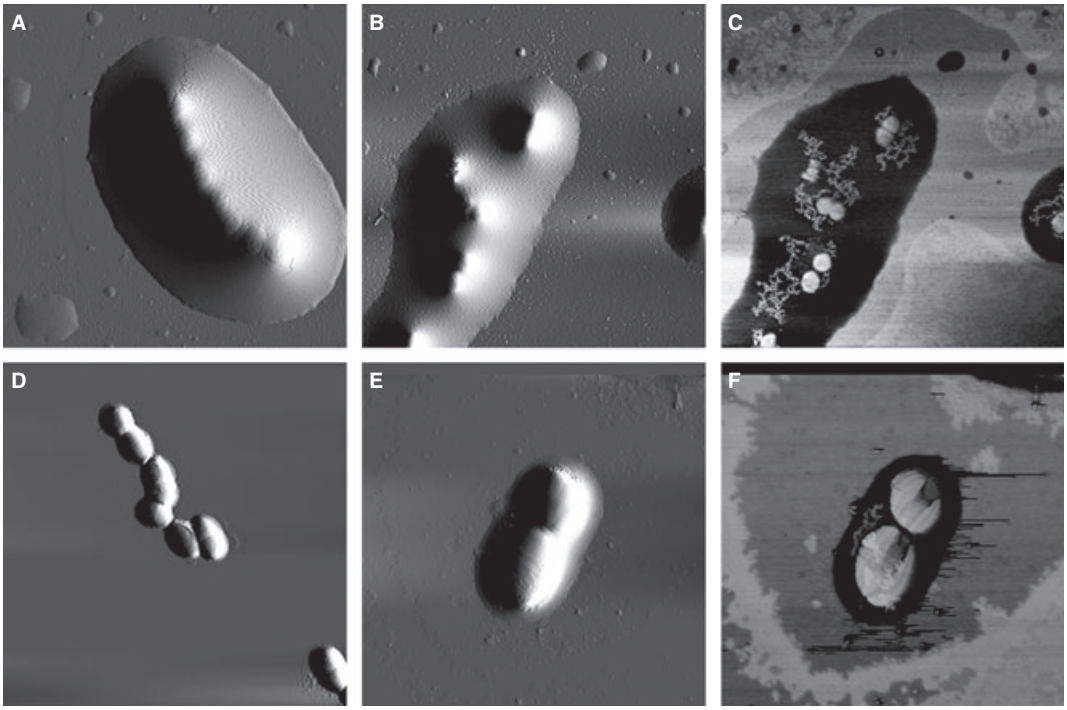

Figure 3 Capsule visualization using atomic force microscopy. Amplitude images (A, B) of wild-type and (D, E) of the MI016 Δ*cps* mutant. Phase image of the (C) wild-type and (F) the MI016 Δ*cps* mutant. The scan size of the images is (A, B, C, D) 10 × 10 μm, or (E, F) 7 × 7 μm.

The capsule deletion mutant shows increased cell surface hydrophobicity

The MATH test was used to quantify the difference in the surface hydrophobicity between *S. mitis* wild-type and the Δ*cps* mutant. The mutant showed approximately two-fold increased adhesion to hexadecane compared with the wild-type, with no difference between cells grown in normal or 5% CO_2-supplemented atmosphere (Fig. 4B).

Growth rate is enhanced in the capsule deletion mutant under normal atmospheric conditions

Previous studies have reported that capsule deletion in *S. pneumoniae* may result in mutants with increased growth rates (Pearce *et al.*, 2002). We wanted to investigate if this was also a phenotypic characteristic of capsule-defective mutants in *S. mitis*. Under normal atmospheric conditions the Δ*cps* mutant had an enhanced growth rate compared with the wild-type, but this difference was not found under 5% CO_2-supplemented conditions (Fig. 4C).

Deletion of the capsule locus in *S. mitis* results in a mutant with increased biofilm formation

The effect of capsule deletion on *S. mitis* surface charge and cell hydrophobicity, both factors associated with the ability of the cells to bind to surfaces, prompted us to investigate whether deletion of the capsule locus affected the biofilm-forming capacity of *S. mitis*. The Δ*cps* mutants constructed with either the erythromycin-resistance (MI015) (data not shown) or the kanamycin-resistance gene cassettes (MI016) showed an increased ability to form biofilm under normal atmospheric conditions supplemented or not with 5% CO_2 compared with the wild-type (Fig. 4D). However, the Δ*cps* formed significantly less biofilm under normal atmospheric conditions than in 5% CO_2-supplemented atmosphere. For the wild-type there were no significant differences between the two growth conditions investigated (Fig. 4D). The SEM images confirmed the increased ability of the Δ*cps* mutant to form biofilm, and revealed that the Δ*cps* mutant formed large aggregates that were not found in the *S. mitis* wild-type (Fig. 5).

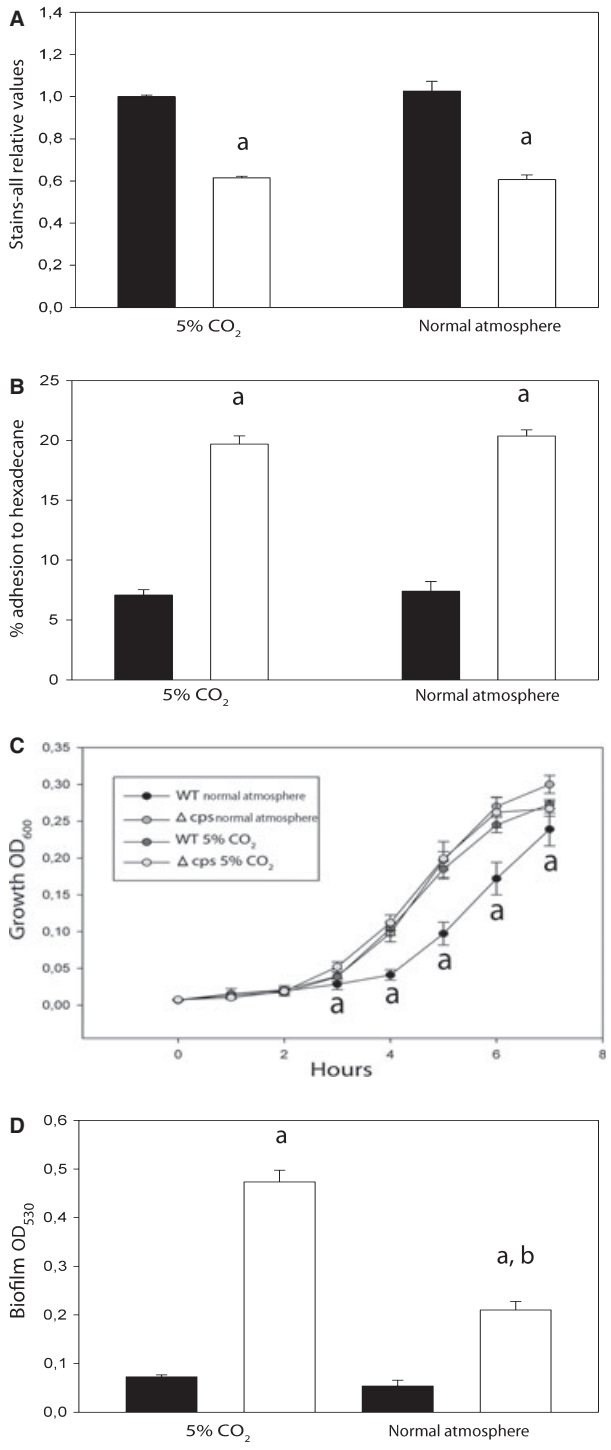

Figure 4 Functional characterization of the *Streptococcus mitis* CCUG 31611^T and the Δ*cps* mutant grown in normal or 5% CO_2 supplemented atmosphere. (A) Surface charge, measured as relative binding to Stains-all. Average values for the wild-type grown in 5% CO_2 were used to normalize the data; (B) hydrophobicity measured as percentage adhesion to hexadecane; (C) growth in normal and 5% CO_2 supplemented atmosphere was recorded as absorbance at 600 nm. (D) Biofilms were quantified by safranin absorbance at 530 nm. Filled bars correspond to *S. mitis* wild-type, and open bars correspond to the Δ*cps* mutant. [a]Significantly different from the wild-type; [b]Significantly different from the Δ*cps* mutant in 5% CO_2. The mean and standard deviation from three independent experiments with two or three parallels are shown ($P < 0.001$).

The capsule deletion mutant shows enhanced autoaggregation

Coaggregation buffer with a concentration of calcium close to what is reported in human whole saliva (Larsen & Pearce, 2003) was used for resuspension of the bacterial cells that were grown overnight in TSB. Examination under phase-contrast microscopy revealed that the Δ*cps* mutant formed larger aggregates (Fig. 6A) that were more sparsely distributed over the glass surface than the wild-type (Fig. 6B). After 1 h there were observable agglomerates of bacteria in the Δ*cps* when gently agitated, which were not present in the wild-type (not shown). Cell density values at OD_{600} were reduced by 12% in the Δ*cps* mutant compared with the wild-type, confirming the increased aggregation of the Δ*cps* mutant observed by microscopy (Fig. 6C).

DISCUSSION

Analysis of the sequenced genomes of six *S. mitis* strains revealed the presence of a putative capsule locus in four of them. The locus had a similar gene arrangement to *S. pneumoniae*, with the conserved *cpsABCDE* genes preceding a set of genes encoding the interstrain variable region involved in capsule production. The differences in the variable region between the different strains suggest that capsule-type variations may also be a characteristic of encapsulated *S. mitis*. It has been suggested that the capsule locus of *S. oralis* is involved in production of receptor polysaccharides (Yang *et al.*, 2009). The receptor polysaccharide resembles the *S. pneumoniae* capsule, but it is usually a teichoic acid with a lectin-binding site involved in coaggregation with other oral bacteria. In *S. mitis*, however, polysaccharides with properties that more closely resemble the *S. pneumoniae* capsule and without the lectin-binding site have been reported, and suggested to represent

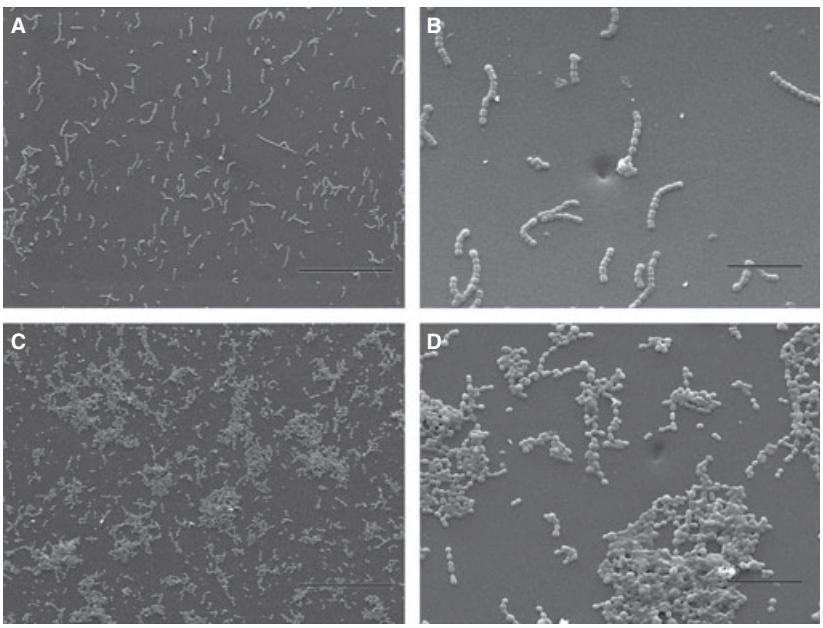

Figure 5 Scanning electron microscopy images showing increased biofilm formation by the MI016 Δ*cps* mutant. (A, B) *S. mitis* wild-type, and (C, D) the Δ*cps* mutant. The bars correspond to (A, B) 50 μm and (B, D) 10 μm.

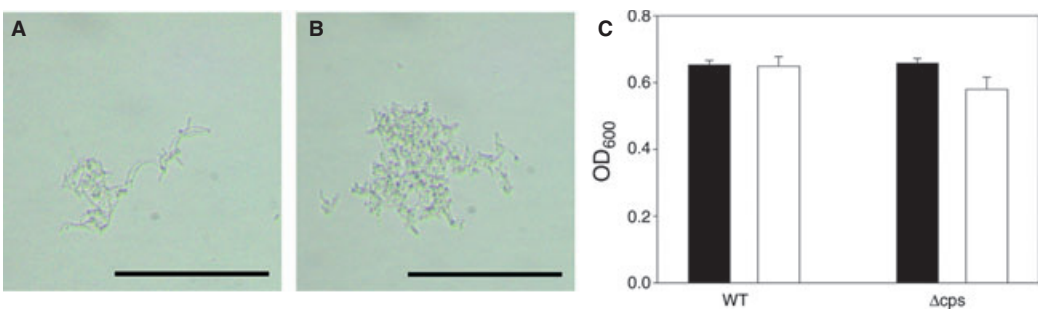

Figure 6 Aggregation of the wild-type and the MI016 Δ*cps* mutant. Light microscopy images of (A) *Streptococcus mitis* wild-type and (B) the Δ*cps* in coaggregation buffer. Optical density values measured immediately after dilution in coaggregation buffer (black bars) or 20 min after dilution in coaggregation buffer (open bars). [a]Significantly different from wild-type immediately and 20 min after dilution in coaggregation buffer and from Δ*cps* immediately after dilution ($P < 0.001$). The mean and standard deviation from three independent experiments were calculated using one-way analysis of variance, followed by the Holm–Sidak test.

a possible equivalent to the *S. pneumoniae* capsule (Bergstrom *et al.*, 2000, 2003; Kilian *et al.*, 2008). Future identification of the nature of the capsule-like structure associated with the *S. mitis* capsule locus may reveal important information on the differences in pathogenic potential between oral streptococci and *S. pneumoniae*.

Mutations in promoter or gene sequences of the capsule locus may potentially affect expression of the capsule. The unencapsulated *S. pneumoniae* R6 strain has, for instance, a capsule locus that is poorly transcribed, most likely because of mutations within the putative capsule promoter sequence (Garcia & Moscoso, 2009). It was important, therefore, to investigate whether the capsule locus was associated with capsule production in *S. mitis*. Consequently, TEM and AFM of the *S. mitis* type strain and its isogenic mutant in which the capsule locus was deleted were used for this purpose. The two techniques involve distinct preparation protocols, and are therefore thought to be complementary. The techniques used for TEM sample preparation were based on the use of ruthenium red and lysine acetate, both thought to stabilize the structure of the negatively charged poly-

saccharides during the dehydration steps (Fassel *et al.*, 1998; Fassel & Edmiston, 1999). This approach revealed a clear capsule-like structure surrounding the *S. mitis* wild-type, whereas this structure could not be identified in the capsule deletion mutant. The results indicated also, that the capsule polysaccharide in *S. mitis* is likely to have a negative charge, because stabilization was obtained with the cationic agent ruthenium red.

The AFM technique for visualization of capsule structures in gram-negative bacteria was recently reported, and it was found to have a higher degree of sensitivity for capsule identification than TEM (Stukalov *et al.*, 2008). Sample preparation for AFM allows visualization of the capsule without the use of dehydration steps, and provides in addition structural three-dimensional information. With this technique, suspension of bacterial cells in HEPES is used with the purpose of stabilizing the capsule structure. This stabilizing effect has been postulated to occur as a result of cross-link interactions between HEPES and the acidic polysaccharides (Suo *et al.*, 2007). The AFM images revealed the presence of *S. mitis* capsule-like structures in the wild-type that were much larger than those observed by TEM. Such differences have also been observed in studies of gram-negative microorganisms (Suo *et al.*, 2007; Stukalov *et al.*, 2008). In the capsule deletion mutant this capsule-like structure was absent, or reduced compared with the *S. mitis* wild-type. The structure observed in some of the cells may be caused by other extracellular polysaccharides, in which the enzymes responsible for their production are not located in the capsule locus. In *S. mitis* a homologous region to the *S. pneumoniae lic1* and *lic2* operon responsible for teichoic acid production is found, for instance, outside the *S. mitis* capsule locus. Phenotypically, the presence of different polysaccharides associated with the cell wall of single *S. mitis* strains (Bergstrom *et al.*, 2000, 2003) support also the contention that polysaccharides in which the synthetic encoding genes are not in the capsule locus may be present in *S. mitis*. The reason why such residual material resembling a capsule-like structure is observed in AFM but not in TEM images is not known, but it may be related to differences in sample preparations, such as absence of fixation in the AFM technique (Stukalov *et al.*, 2008).

The charge and the hydrophobicity of the bacteria are important for adhesion to host components and to other bacteria. Weak electrostatic forces are involved in the initial attachment, followed by more specific receptor–ligand interactions when intimate contact is established (Cowan *et al.*, 1987; Nobbs *et al.*, 2009). Cell surface charge may also affect the response of two component signal transduction systems and gene expression (Hyyrylainen *et al.*, 2007). We examined, therefore, whether these properties are also associated with capsule-like production in *S. mitis*. In *S. pneumoniae*, deletion of the capsule locus is generally associated with an increase in hydrophobicity and a reduction in the overall surface charge (Granlund-Edstedt *et al.*, 1993; Swiatlo *et al.*, 2002). As discussed above, the visualization of the *S. mitis* capsule-like structure using ruthenium red during sample preparation, suggested that the capsule-like structure was likely to contribute to the negative charge of *S. mitis*. To quantify such an effect, we used Stains-all, a positively charged molecule that binds to the generally negatively charged capsule (Schrager *et al.*, 1996; Magee & Yother, 2001). The results showed that the capsule locus deletion mutant bound less Stains-all than the wild-type, underlying the overall negative charge of the capsule-like material.

We report here that the *S. mitis* capsule locus deletion mutant had an increased adsorption to hexadecane, which is interpreted as an increase in hydrophobicity (Rosenberg *et al.*, 1980). The hydrophobicity of bacteria and streptococci has been linked to adhesion to various surfaces. In the multiple-site model of adhesion to hydroxyapatite, hydrophobicity is an important contributing factor for adhesion (Doyle *et al.*, 1982). Hydrophobicity has also been linked to adhesion to biomaterials (Fujioka-Hirai *et al.*, 1987; Satou *et al.*, 1988) and increased binding to epithelial cells (Weerkamp *et al.*, 1987). The enhanced biofilm-forming capacity may be related, at least in part, to the changes in surface charge and hydrophobicity discussed above. It is also possible that differences in growth patterns may also contribute to such differences, as we found out that the deletion mutant may have a slight increase in growth rate. The growth advantage in mutants lacking capsule have also been observed in *S. pneumoniae* (Pearce *et al.*, 2002).

The deletion of the capsule locus was associated with increased aggregation levels in CAB. The calcium concentration in the CAB is close to the reported calcium level found in human whole saliva,

and calcium is reported to have a pivotal role in aggregation of oral bacteria (Cisar *et al.*, 1979). The increased aggregation observed for the Δ*cps* mutant might be caused by more intimate contact between the bacteria in the absence of capsule, possibly through exposure of surface proteins that may participate in binding to other cells. The increased hydrophobicity of the Δ*cps* mutant may also be a factor contributing to the increased aggregation observed (McNab *et al.*, 1999). Aggregation plays also most probably an important factor in biofilm formation (Kolenbrander *et al.*, 2010). The SEM images showed that *S. mitis* biofilms exhibited cell aggregates, despite the fact that in the medium used for the biofilm formation no clear aggregates were observed in planktonic cells (data not shown). It is interesting that in *S. pneumoniae*, a similar enhancing effect on biofilm formation has been observed in capsule deletion mutants (Munoz-Elias *et al.*, 2008). The authors observed, in addition, that the involvement of surface proteins on pneumococcal biofilm was apparent only in the capsule deletion mutants, indicating that the capsule may hinder access of surface proteins to their ligands (Munoz-Elias *et al.*, 2008). It has also been postulated that reduced capsule production is important for the initial attachment of *S. pneumoniae* during biofilm formation and pathogenesis, and plays an important role in initial colonization (Domenech *et al.*, 2009). Our observation that the capsule locus deletion mutant formed less biofilm during growth in normal atmospheric conditions than under 5% supplemented CO_2, and that this effect could not be observed for the wild-type, underline the finding that phenotypic effects on biofilm formation are more pronounced in unencapsulated mutants.

In this study we focused on functions of the *S. mitis* capsule locus associated with surface properties and biofilm formation. Such functions are particularly relevant for *S. mitis* because they are predominantly early colonizers of tooth surfaces, forming the basis to which more pathogenic bacteria may be able to join oral biofilms. *Streptococcus mitis* is, however, also a common colonizer of the throat, where *S. pneumoniae* is usually present. In *S. pneumoniae*, the capsule plays an important role in resistance to phagocytosis, with the capsule serotype reported to be more important than the genetic background (Melin *et al.*, 2010). It will be interesting, therefore, to investigate how the possible different capsular-like types of the commensal *S. mitis* may differ in their potential to be phagocytosed compared with invasive *S. pneumoniae*.

ACKNOWLEDGEMENTS

We thank Heidi Aarø Åmdal for laboratory assistance, Yiqing Cai for help with the transmission electron microscopy and Steinar Stølen for help with the scanning electron microscopy. We are grateful for the available drafts of the genomes of *S. mitis* (JCVI, and Institute for Genome Sciences, University of Maryland School of Medicine).

REFERENCES

Aas, J.A., Paster, B.J., Stokes, L.N., Olsen, I. and Dewhirst, F.E. (2005) Defining the normal bacterial flora of the oral cavity. *J Clin Microbiol* **43**: 5721–5732.

Beighton, D., Carr, A.D. and Oppenheim, B.A. (1994) Identification of viridans streptococci associated with bacteremia in neutropenic cancer-patients. *J Med Microbiol* **40**: 202–204.

Beisswenger, C., Coyne, C.B., Shchepetov, M. and Weiser, J.N. (2007) Role of p38 MAP kinase and transforming growth factor-beta signaling in transepithelial migration of invasive bacterial pathogens. *J Biol Chem* **282**: 28700–28708.

Bentley, S.D., Aanensen, D.M., Mavroidi, A. *et al.* (2006) Genetic analysis of the capsular biosynthetic locus from all 90 pneumococcal serotypes. *Plos Genetics* **2**: 262–269.

Bergstrom, N., Jansson, P.E., Kilian, M. and Sorensen, U.B.S. (2000) Structures of two cell wall-associated polysaccharides of a *Streptococcus mitis* biovar 1 strain – a unique teichoic acid-like polysaccharide and the group O antigen which is a C-polysaccharide in common with pneumococci. *Eur J Biochem* **267**: 7147–7157.

Bergstrom, N., Jansson, P.E., Kilian, M. and Sorensen, U.B.S. (2003) A unique variant of streptococcal group O-antigen (C-polysaccharide) that lacks phosphocholine. *Eur J Biochem* **270**: 2157–2162.

Bogaert, D., De Groot, R. and Hermans, P.W. (2004) *Streptococcus pneumoniae* colonisation: the key to pneumococcal disease. *Lancet Infect Dis* **4**: 144–154.

Cisar, J.O., Kolenbrander, P.E. and McIntire, F.C. (1979) Specificity of coaggregation reactions between human oral streptococci and strains of *Actinomyces viscosus* or *Actinomyces naeslundii*. *Infect Immun* **24**: 742–752.

Cowan, M.M., Taylor, K.G. and Doyle, R.J. (1987) Energetics of the initial phase of adhesion of *Streptococcus sanguis* to hydroxylapatite. *J Bacteriol* **169**: 2995–3000.

Denapaite, D., Bruckner, R. and Nuhn, M., *et al.* (2010) The genome of *Streptococcus mitis* B6–what is a commensal? *PLoS One* **5**: e9426.

Domenech, M., Garcia, E. and Moscoso, M. (2009) Versatility of the capsular genes during biofilm formation by *Streptococcus pneumoniae*. *Environ Microbiol* **11**: 2542–2555.

Doyle, R.J., Nesbitt, W.E. and Taylor, K.G. (1982) On the mechanism of adherence of *Streptococcus sanguis* to hydroxyapatite. *FEMS Microbiol Lett* **15**: 1–5.

Fassel, T.A. and Edmiston, C.E. (1999) Ruthenium red and the bacterial glycocalyx. *Biotechn Histochem* **74**: 194–212.

Fassel, T.A., Mozdziak, P.E., Sanger, J.R. and Edmiston, C.E. (1998) Superior preservation of the staphylococcal glycocalyx with aldehyde-ruthenium red and select lysine salts using extended fixation times. *Microsc Res Techn* **41**: 291–297.

Fujioka-Hirai, Y., Akagawa, Y., Minagi, S. *et al.* (1987) Adherence of *Streptococcus mutans* to implant materials. *J Biomed Mat Res* **21**: 913–920.

Garcia, E. and Moscoso, M. (2009) Transcriptional regulation of the capsular polysaccharide biosynthesis locus of *Streptococcus pneumoniae*: a bioinformatic analysis. *DNA Res* **16**: 177–186.

Granlund-Edstedt, M., Sellin, M., Holm, A. and Hakansson, S. (1993) Adherence and surface properties of buoyant density subpopulations of group B streptococci, type III. *Acta Pathol Microbiol Immunol Scand* **101**: 141–148.

Hammerschmidt, S., Wolff, S., Hocke, A. *et al.* (2005) Illustration of pneumococcal polysaccharide capsule during adherence and invasion of epithelial cells. *Infect Immun* **73**: 4653–4667.

Hammerschmidt, S., Agarwal, V., Kunert, A. *et al.* (2007) The host immune regulator factor H interacts via two contact sites with the PspC protein of *Streptococcus pneumoniae* and mediates adhesion to host epithelial cells. *J Immunol* **178**: 5848–5858.

Hyyrylainen, H.L., Pietiainen, M., Lunden, T. *et al.* (2007) The density of negative charge in the cell wall influences two-component signal transduction in *Bacillus subtilis*. *Microbiology* **153**: 2126–2136.

Johnston, C., Hinds, J., Smith, A. *et al.* (2010) Detection of large numbers of pneumococcal virulence genes in streptococci of the mitis group. *J Clin Microbiol* **48**: 2762–2769.

Kadioglu, A., Weiser, J.N., Paton, J.C. and Andrew, P.W. (2008) The role of *Streptococcus pneumoniae* virulence factors in host respiratory colonization and disease. *Nat Rev Microbiol* **6**: 288–301.

Kilian, M., Poulsen, K., Blomqvist, T. *et al.* (2008) Evolution of *Streptococcus pneumoniae* and its close commensal relatives. *PLoS ONE* **3**: e2683.

Kim, J.O. and Weiser, J.N. (1998) Association of intrastrain phase variation in quantity of capsular polysaccharide and teichoic acid with the virulence of *Streptococcus pneumoniae*. *J Infect Dis* **177**: 368–377.

Kim, J.O., Romero-Steiner, S., Sorensen, U.B.S. *et al.* (1999) Relationship between cell surface carbohydrates and intrastrain variation on opsonophagocytosis of *Streptococcus pneumoniae*. *Infect Immun* **67**: 2327–2333.

Kolenbrander, P.E. and London, J. (1993) Adhere today, here tomorrow – oral bacterial adherence. *J Bacteriol* **175**: 3247–3252.

Kolenbrander, P.E., Palmer, R.J. Jr, Periasamy, S. and Jakubovics, N.S. (2010) Oral multispecies biofilm development and the key role of cell-cell distance. Nature reviews. *Microbiology* **8**: 471–480.

Larsen, M.J. and Pearce, E.I. (2003) Saturation of human saliva with respect to calcium salts. *Archiv Oral Biol* **48**: 317–322.

Lau, P.C., Sung, C.K., Lee, J.H., Morrison, D.A. and Cvitkovitch, D.G. (2002) PCR ligation mutagenesis in transformable streptococci: application and efficiency. *J Microbiol Meth* **49**: 193–205.

Lee, M.S. and Morrison, D.A. (1999) Identification of a new regulator in *Streptococcus pneumoniae* linking quorum sensing to competence for genetic transformation. *J Bacteriol* **181**: 5004–5016.

Levitz, R.E. (1999) Prosthetic-valve endocarditis caused by penicillin-resistant *Streptococcus mitis*. *N Engl J Med* **340**: 1843–1844.

Li, J., Helmerhorst, E.J., Leon, C.W. *et al.* (2004) Identification of early microbial colonizers in human dental biofilm. *J Appl Microbiol* **97**: 1311–1318.

Lyons, E. and Freeling, M. (2008) How to usefully compare homologous plant genes and chromosomes as DNA sequences. *Plant J* **53**: 661–673.

Macfarlane, S., Ledder, R.G., Timperley, A.S., Friswell, M.K. and McBain, A.J. (2008) Coaggregation between and among human intestinal and oral bacteria. *FEMS Microbiol Ecol* **66**: 630–636.

MacLeod, C.M. and Krauss, M.R. (1950) Relation of virulence of pneumococcal strains for mice to the quantity

of capsular plysaccharide formed in vitro. *J Exp Med* **92**: 1–9.

Magee, A.D. and Yother, J. (2001) Requirement for capsule in colonization by *Streptococcus pneumoniae*. *Infect Immun* **69**: 3755–3761.

Marron, A., Carratala, J., Gonzalez-Barca, E. *et al.* (2000) Serious complications of bacteremia caused by viridans streptococci in neutropenic patients with cancer. *Clin Infect Dis* **31**: 1126–1130.

Mavroidi, A., Aanensen, D.M., Godoy, D. *et al.* (2007) Genetic relatedness of the *Streptococcus pneumoniae* capsular biosynthetic loci. *J Bacteriol* **189**: 7841–7855.

McNab, R., Forbes, H., Handley, P.S. *et al.* (1999) Cell wall-anchored CshA polypeptide (259 kilodaltons) in *Streptococcus gordonii* forms surface fibrils that confer hydrophobic and adhesive properties. *J Bacteriol* **181**: 3087–3095.

Melin, M., Trzcinski, K., Meri, S., Kayhty, H. and Vakevainen, M. (2010) The capsular serotype of *Streptococcus pneumoniae* is more important than the genetic background for resistance to complement. *Infect Immun* **78**: 5262–5270.

Munoz-Elias, E.J., Marcano, J. and Camilli, A. (2008) Isolation of *Streptococcus pneumoniae* biofilm mutants and their characterization during nasopharyngeal colonization. *Infect Immun* **76**: 5049–5061.

Nelson, A.L., Roche, A.M., Roche, J.M. *et al.* (2007) Capsule enhances pneumococcal colonization by limiting mucus-mediated clearance. *Infect Immun* **75**: 83–90.

Nobbs, A.H., Lamont, R.J. and Jenkinson, H.F. (2009) Streptococcus adherence and colonization. *Microbiol Mol Biol Rev* **73**: 407–450.

Pearce, C., Bowden, G.H., Evans, M. *et al.* (1995) Identification of pioneer viridans streptococci in the oral cavity of human neonates. *J Med Microbiol* **42**: 67–72.

Pearce, B.J., Iannelli, F. and Pozzi, G. (2002) Construction of new unencapsulated (rough) strains of *Streptococcus pneumoniae*. *Res Microbiol* **153**: 243–247.

Petersen, F.C. and Scheie, A.A. (2010) Natural transformation of oral streptococci. *Meth Mol Biol* **666**: 167–180.

Petersen, F.C., Tao, L. and Scheie, A.A. (2005) DNA binding-uptake system: a link between cell-to-cell communication and biofilm formation. *J Bacteriol* **187**: 4392–4400.

Pfaffl, M.W., Horgan, G.W. and Dempfle, L. (2002) Relative expression software tool (REST) for group-wise comparison and statistical analysis of relative expression results in real-time PCR. *Nucleic Acids Res* **30**: e36.

Rosenberg, M., Gutnick, D. and Rosenberg, E. (1980) Adherence of bacteria to hydrocarbons – a simple method for measuring cell-surface hydrophobicity. *FEMS Microbiol Lett* **9**: 29–33.

Sabella, C., Murphy, D. and Drummond-Webb, J. (2001) Endocarditis due to *Streptococcus mitis* with high-level resistance to penicillin and ceftriaxone. *J Am Med Assoc* **285**: 2195–2195.

Satou, J., Fukunaga, A., Satou, N., Shintani, H. and Okuda, K. (1988) Streptococcal adherence on various restorative materials. *J Dent Res* **67**: 588–591.

Schrager, H.M., Rheinwald, J.G. and Wessels, M.R. (1996) Hyaluronic acid capsule and the role of streptococcal entry into keratinocytes in invasive skin infection. *J Clin Invest* **98**: 1954–1958.

Stukalov, O., Korenevsky, A., Beveridge, T.J. and Dutcher, J.R. (2008) Use of atomic force microscopy and transmission electron microscopy for correlative studies of bacterial capsules. *Appl Environ Microbiol* **74**: 5457–5465.

Suo, Z., Yang, X., Avci, R. *et al.* (2007) HEPES-stabilized encapsulation of *Salmonella typhimurium*. Langmuir : the ACS. *J Surf Coll* **23**: 1365–1374.

Swiatlo, E., Champlin, F.R., Holman, S.C., Wilson, W.W. and Watt, J.M. (2002) Contribution of choline-binding proteins to cell surface properties of *Streptococcus pneumoniae*. *Infect Immun* **70**: 412–415.

Tunkel, A.R. and Sepkowitz, K.A. (2002) Infections caused by viridans streptococci in patients with neutropenia. *Clin Infect Dis* **34**: 1524–1529.

Weerkamp, A.H., Vandermei, H.C. and Slot, J.W. (1987) Relationship of cell-surface morphology and composition of *Streptococcus salivarius* K+ to adherence and hydrophobicity. *Infect Immun* **55**: 438–445.

Weinberger, D.M., Trzcinski, K., Lu, Y.J. *et al.* (2009) Pneumococcal capsular polysaccharide structure predicts serotype prevalence. *PLoS Pathogens* **5**: e1000476.

Yang, J., Ritchey, M., Yoshida, Y., Bush, C.A. and Cisar, J.O. (2009) Comparative structural and molecular characterization of ribitol-5-phosphate-containing *Streptococcus oralis* coaggregation receptor polysaccharides. *J Bacteriol* **191**: 1891–1900.